



Full Length Article

Nanocellulose as an inhibitor of water-in-crude oil emulsion formation

Maria M. González, Cristian Blanco-Tirado, Marianny Y. Combariza*



Escuela de Química, Universidad Industrial de Santander, Bucaramanga 680002, Colombia

ARTICLE INFO

Keywords:
 Nanocellulose
 W/o emulsion
 Inhibition
 Crude oil

ABSTRACT

Formation of water/oil emulsions is a frequent and challenging problem to deal with during crude oil extraction and processing. Crude oil must have water contents (BS&W) below 0,5% to meet transport and export requirements. Lowering BS&W values in crude oils involve physical and chemical processes or their combinations. Chemical demulsifiers, particularly, are structurally diverse and predominantly petrochemically-derived; however, alternative surface-active compounds such as biosurfactants are nowadays the topic of active research. In this contribution, we report the use of aqueous suspensions of cellulose nanoparticles, both nanocrystals (CNC) and nanofibrils (CNF), to inhibit the formation of w/o emulsions. HLB values of 13.0 for CNF and 10.7 for CNC indicate that these materials are hydrophilic o/w emulsifying agents, and as such can also act as destabilizers for w/o emulsions. We observe, by recovered water and Near-Infrared (NIR) scattering measurements, that CNC and CNF can effectively function as inhibitors of synthetic w/o and natural w/crude oil emulsions. Aqueous suspensions of CNC and CNF decrease the amount of emulsified water, inhibiting the formation of w/o emulsions up to 75% in some cases.

1. Introduction

Stable water-in-oil emulsions form between hydrocarbons and formation water due to high-energy mixing conditions during crude oil extraction and pumping. Also, the presence of naphthenic acids and other surface-active compounds found in asphaltenes and resins increase the stability of these emulsions [1]. Similarly, in the case of non-conventional fossil fuel sources, the use of enhanced recovery (EOR) techniques where mixtures of surfactants and polymers are used to extract the oil, aggravate the issue of emulsion formation.

Before transport and processing, water is removed from the crude oil by demulsification to avoid issues such as increased viscosity, corrosion, and salt deposits formation in pipelines and catalyst poisoning in refining schemes. Demulsification of crude oils is typically carried out through physical, biological, and chemical methods or their combinations [2–4]. The use of chemical methods is widespread due to the low cost and convenience of application of surfactants and demulsifiers. These substances (petrochemically-derived in most cases) are known as emulsion inhibitors or emulsion breakers if applied before or after emulsion formation, respectively. In general, commercially available additives for inhibiting or breaking emulsions are mixtures of synthetic surfactants with known negative environmental impact.

Back in 1995, Dalmazzone et al developed a methodology to study the action of emulsion inhibitors and breakers. In this study an inhibitor

is defined as a surfactant added before the oil water mixture is performed, and the percentage of recovered water is reported as a percentage of inhibition; whereas, when the agent is added after the emulsion is formed it is considered a demulsifier [5]. The inhibition or separation of the aqueous and oily phases of an emulsion is achieved by changing the hydro-lipophilic balance (HLB) of the surfactant added to the system. The effect of inhibitors and demulsifiers is achieved because they compete for the interface against surfactants naturally present in samples. In the case of water-in-crude oil emulsions, natural surfactants are mainly asphaltenes, naphthenic acids, and resins [6,7]. More recently, Hjartnes et al. discuss how in oil processing chemical treatment of emulsions involves the use of non-emulsifiers and demulsifiers. Non-emulsifiers (or inhibitors) are added almost exclusively to the oil to avoid emulsion formation during production, transport and process; hence, these materials have hydrophobic properties represented by low HLB values. Demulsifiers, on the other hand, are used to break already formed w/o or o/w emulsions [6]. Regardless of the type of agent, most inhibitors or demulsifiers currently in use are synthetic, petroleum-derived materials.

Nowadays, trends in sustainable development promote the use of renewable sources of materials, in place of synthetic raw sources for new products, to change the current Linear Economy model. Within this framework, lignocellulosic biomass, derived from intensive agro-industrial activity, emerges as an attractive raw material because of its

* Corresponding author.

E-mail address: marianny@uis.edu.co (M.Y. Combariza).

availability and low cost. Production and usage of advanced nanocellulose materials (nanocrystals or nanofibrils – CNC, CNF) from biomass is currently an active research and innovation topic [9–12]. Sulfuric acid hydrolysis and TEMPO-oxidation are the main processes for CNC and CNF production, respectively, and many researchers reported optimized conditions for these methods such as Bodenson *et al.* [13] and Saito *et al.* [14].

CNC has many applications in medicine (biomedical implants, pharmaceuticals) and material sciences (Pickering emulsions, antimicrobial films, reinforcing fillers for polymers, flexible displays, oil absorbents, fabric, and textiles) [15–18]. Several studies concerning the use of cellulose as a surface-active agent exist in the scientific literature. For instance, Andersen *et al.* [19] examining the ability of microfibrillated cellulose for stabilizing oil in water emulsions found that increasing the hydrophobicity of the biopolymer resulted in an increased surfactant activity. Lif *et al.* [20] also reported the use of microfibrillated cellulose with different degrees of hydrophobicity to stabilize water-diesel emulsions and determined that using a mixture of hydrophobic and hydrophilic microfibrillated cellulose provided efficient stabilization of the emulsion.

Furthermore, Hou *et al.* [21] showed that ethyl-cellulose could be used to destabilize water/bitumen emulsions. Also, some reports indicate the use of hydrophobic nanocellulose for stabilizing Pickering emulsions in food, cosmetic formulations, and pharmaceuticals, [22–26]. Usually, for Pickering emulsions concentrations of nanocellulose range from 0.1 to 1.5%. TEMPO nanofibrils (TOCN) produce more stable emulsions than CNC, probably due to network formation as a result of longer fibril length and increased ionic charge, in comparison with nanocrystals. [27]. On the other hand, studies of emulsion stabilization using hydrolyzed cellulose showed that increasing hydrolysis times results in smaller cellulosic particles, which in turn produce stable o/w emulsions by decreasing drop size [28,29].

The use of nanocellulose in fluids for EOR processes has also been reported. For instance, surface modified cellulose nanofibrils containing hydrophobic alkyl units were used as emulsifiers to increase the amount of extractable crude [30] in experimental micromodels. On another application, Wei *et al.* used CNF solutions (0.2 and 0.5%) to change source rocks wettability, to water-wet, and allow crude oil extraction by inducing the formation of w/o emulsions [31,32]. Also, Lia *et al.* found that hydrophobization of CNC increases thermal stability, hinders aggregation in the presence of electrolytes, and reduces viscoelasticity of the materials. All of these properties are of fundamental importance in EOR processes [33]. Nanocellulose-based additives can also be used as foam stabilizers in foam-flooding EOR strategies, by reducing oil/water interfacial tension and promoting oil displacement in the source rock [28–36]. Also, CNC can cross sandstone nuclei and alter mineral surfaces properties to allow crude migration and efficient extraction [36,37]. Besides, the stability of CNC suspensions is not affected by pH changes or high temperatures (90 °C), which is of fundamental importance for crude oil recovery applications [38].

In this contribution our rationale involves a simple assumption: If a hydrophilic (water-soluble) surfactant with high HLB is able to stabilize o/w emulsions, then the same type of material could hinder the formation of w/o emulsions. In fact, Roodbari *et al.* demonstrated how a group of non-ionic polymers (Tweens analogues), typically used to stabilize o/w emulsions, exhibit destabilizing properties in w/crude oil mixtures. The authors reported that the demulsification effect increases as the HLB of the surfactant increases, and also as the number of electronegative atoms (oxygen) increase in the molecules. These surfactants were able to recover up to 80% water from the w/crude oil emulsion. However, the authors used the Tweens as demulsifiers by adding them once the w/o emulsion was formed [8]. Currently, high-molecular-weight (HMW) surfactants are attracting a lot of attention as demulsifiers in w/o emulsions. For instance, Wang *et al.* using polyethoxylated dendrimers as demulsifiers and found that the amount of recovered water increases as the numbers of propylene oxide and

ethylene oxide units increase. These HMW are believed to alter interfacial water/oil film rheology promoting coalescence and sedimentation [68]. We hypothesize that highly hydrophilic nanocelluloses, with abundant oxygen atoms, high-molecular-weight, and high HLB values, can efficiently inhibit w/o emulsion formation.

Thus, here we investigate the role of cellulose nanoparticles -nanocrystals (CNC) and nanofibrils (CNF) obtained by acid hydrolysis and TEMPO, respectively- as surface active agents for inhibiting water in oil emulsion formation. An aqueous carrier phase containing CNC and CNF with different amounts of active surface groups (SO₃⁻ and COOH⁻, respectively) was mixed with the non-polar phase employing a high shear mixer. We observed a dramatic decrease in the amount of emulsified water when the aqueous carrier contained above 1000 ppm of nanocellulose. In this way, the use of activated CNC suspensions can decrease the amount of emulsified water in w/o systems. Besides, the use of biodegradable polymers can reduce the environmental impacts associated with synthetic additives commonly used to break w/o emulsions in the petroleum industry.

2. Experimental and methods

2.1. Materials

Sulfuric acid (H₂SO₄), sodium hydroxide (NaOH), sodium bromide (NaBr), hydrochloric acid (HCl, 37% weight), sodium hypochlorite (NaClO, 5–9% chlorine) and ethanol (95%) were purchased from Merck (Darmstadt, Germany). TEMPO (2,2,6,6-tetramethyl-piperidine-1-oxyl, 98%) and Grade 1 Whatman cellulose filters were acquired from Sigma Aldrich (St. Louis, MO, USA). Microcrystalline cellulose was purchased from Alfa Aesar (Ward Hill, Massachusetts, United States). All chemical reagents were used as supplied. Commercial-grade diesel and gasoline were also used as received. Aqueous solutions and suspensions were prepared with ultrapure water (12 MΩ·cm @ 25 °C).

2.2. CNC isolation by hydrolysis

Typically, cellulose nanocrystals (CNC) extraction involves the removal of amorphous cellulose from bleached fibers via acid hydrolysis. CNCs were prepared via acid hydrolysis, according to Bodenson *et al.* [13], using Whatman filters as cellulose source (5 g) and H₂SO₄ (60 mL, 62.5%). The cellulose-acid mixture was allowed to react at 45 °C for 130 min. After the reaction was stopped, by adding cold water, the mixture was centrifuged and washed until pH 1. Dialysis using a Spectra Dialysis membrane (12–14 kDa) was conducted for six days to remove cellulosic reaction residues. The dialysate was subjected to ultrasonic radiation using a Sonics Vibra Cell VC (20 kHz, 750 W) for 20 min in an ice water bath. Finally, the CNC suspension was lyophilized and stored for further characterization and use in emulsion inhibition tests.

2.3. CNF isolation by TEMPO

Carboxylated cellulose nanofibrils (CNF) were prepared according to the procedure described by Isogai *et al.* [12]. In short, microcrystalline cellulose (1 g) was dispersed in deionized water (100 mL), and catalytic amounts of TEMPO (16 mg) and NaBr (100 mg) were added to the suspension under stirring at room temperature. The reaction mixture was placed on an ultrasonic bath (Bransonic, 40 kHz, 130 Watt) and a solution of NaClO, used as primary oxidant (2 mmol), was added dropwise while the pH of the mixture was kept between 10 and 11, by adding NaOH (0.1 M) when required. When there was no pH change, the reaction was quenched by ethanol addition. The reaction mixture was then centrifuged and washed with water repeatedly, until pH 7. Aqueous suspensions (1% w) of CNF were sonicated by ten-minute cycles (Sonics Vibra-cell VC750, 20 kHz, 750 Watt) to achieve uniform dispersion of the material. The suspensions were centrifuged at 4700 rpm (4643*g) for 20 min to remove unreacted cellulose. Finally,

the dispersed CNF (1%), in the form of sodium carboxylate, was transformed into the free acid form by adding HCl (0,1 M) until pH 2. The mixture was left to react 30 min, under constant stirring, according to Fujisawa et al. [39]. Free carboxylate CNF appeared as a translucent gel.

2.4. CNC and CNF characterization

TEM images were collected on a FEI Tecnai T12 Spirit TEM (FEI, Hillsboro, OR) with an acceleration voltage of 120 keV. Samples for TEM imaging were drop casted onto carbon coated copper grids and left to dry at ambient conditions. X-Ray diffraction patterns were measured on a Bruker D8 DISCOVER X-ray diffractometer (Billerica, MA) with a DaVinci geometry, equipped with a CuK α 1 radiation source (40 kV and 30 mA), an area detector VANTEC-500, and a poly(methyl methacrylate) sample holder. Attenuated total reflectance (ATR-IR) measurements were performed on a Bruker Tensor 27 (Billerica, MA) FTIR instrument equipped with a Platinum Diamond ATR unit A225/Q (Billerica, MA) with a resolution of 2 cm $^{-1}$ and scan accumulation of 32 per spectrum. CNC and CNF thermal stability were tested on a TA Discovery TGA (Newcastle, England) instrument equipped with an infrared heating oven, and a temperature controlled thermobalance, a gas supply module, and an autosampler system. TGA analysis was carried out with Nitrogen as an inert gas (50 mL/min) and a heating rate of 10° C/min from 30 to 600 °C. Finally, the colloidal stability of CNC and CNF aqueous suspensions (1% wt) was assessed according to their zeta potential value (ζ) determined with a Malvern Zetasizer Nano ZS90 instrument (Worcestershire, UK), equipped with a capillary cell 1070. Conductometric titrations were performed using a HANNA H1 8733 conductometer, to assess the number of sulfate groups on the CNC surface and the carboxylic groups on nanofibrils surface. The titrations were performed using a CNC suspension (100 mL, 2 g/L), initially subjected to sonication for 15 min, to which a solution of NaCl (2 mL, 0,05 M) was added. Titration was carried out by adding 10 μ L aliquots of NaOH 0,0197 N under continuous stirring, according to the procedure previously reported by Abitbol [40]. Nanocellulose degree of oxidation was determined by the method described by Habibi et al. [41]. The size of the nanocrystals was determined by Dynamic Light Scattering using a Zetasizer Nano Series S90 Malvern.

Also, for theoretical HLB values, we used the Daviés [42] method, as shown in Eq. (1):

$$\text{HLB} = 7 + \sum \text{HLB}_{\text{Hydrophilic groups}} - \sum \text{HLB}_{\text{Hydrophobic groups}} \quad (1)$$

2.5. Preparation of model emulsions

Synthetic stable w/o emulsions were prepared by mixing a solution of commercial gasoline plus asphaltenes (non-polar phase + surfactant) and brine (pH 6) with a composition similar to that of the average formation water (0,3088 mg/L KCl, 9,93 mg/L NaCl, and 2,52 mg/L CaCl₂·2H₂O) [43]. The brine was spiked with CNC or CNF to achieve concentrations from 500 up to 1500 ppm. A 10000 ppm asphaltene stock solution in toluene was used as surface-active material for w/o emulsions formation; the asphaltenes were mixed with the gasoline to reach concentrations of 1000 ppm with respect to the total volume of the mixture. The asphaltenes were isolated from a South American crude oil API 31,7° according to the ASTM D6560-12 procedure.

For emulsions preparation, 20 mL of the aqueous phase (with and without CNC and CNF) was added dropwise to 20 mL of the organic phase (Ultraturrax T-25 at 13000 rpm) to reach 50% of water content. The type of emulsion was confirmed by wettability tests in pure water and toluene. Since all the emulsions prepared easily dissolved in toluene, they were cataloged as w/o. Micrographs were taken to confirm the formation of w/o emulsions. All w/o emulsions prepared were stable for up to 12 months.

The previous procedure also applied to the preparation of w/o

emulsions with two crude oils. In these emulsions, the gasoline/asphaltene mixture was replaced by crude oils (API: 31.7° and 13.7°). Brines were prepared with concentrations of 1000, 6000 and 12000 ppm of NaCl. The pH values were adjusted by the addition of 0,01 M HCl and 0,01 M NaOH to the brine as required, to obtain values of 6 and 10. All tests were carried out at room temperature.

2.6. Emulsion characterization

The stability of the emulsions was determined by visual inspection (measuring recovered water volume using graduated cylinders) and Near-Infrared (NIR) scattering via the Turbiscan Lab instrument (Formulaction, L'Union, and France). The Turbiscan Lab instrument follows variations in backscattered or transmitted radiation (NIR, λ 850 nm) vs. sample height as a function of time to yield dispersion stability data. The backscattering mode is commonly used to study opaque dispersions such as crude oil emulsions. Eq. (2) shows the Instability Index, a statistical parameter calculated from variations in backscattering intensity of the sample, relative to the original, over time. This index is a convenient way to observe the dynamics of aggregation processes and emulsion stability [44].

$$\text{InstabilityIndex} = \frac{\sum_0^n |BS_i - BS_{i-1}|}{n} \quad (2)$$

where BS_(i) and BS_(i-1) are the dimensionless backscattering value for each scan and n is the number of scans. High values of Instability Index indicate a high probability of phase separation, which translates into low emulsion stability in the case of w/o emulsions [45].

3. Results and discussion

3.1. Nanocellulose surface chemistry and structure

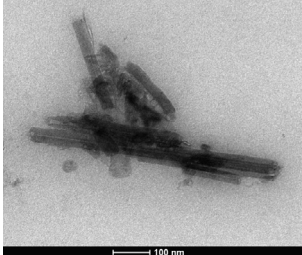
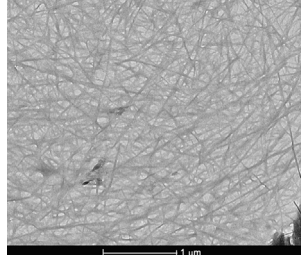
CNC and CNF behavior at interfaces (self-assembly, adsorption, solvent interactions, among others) depends on two key parameters: surface chemistry and particle structure. In CNC and CNF, the isolation methods (e.g., polar/charged surfaces if isolated via H₂SO₄ acid hydrolysis or TEMPO) or specific surface modifications (e.g., hydrophobization reactions) determine their surface properties. Regarding particle structure, nanocelluloses are considered as one-dimensional particles due to the biopolymer's unidirectional biosynthetic pathway [46-48].

We obtained CNC, via acid hydrolysis from Whatman filter paper, with lengths between 100 and 300 nm and widths up to 30 nm, exhibiting a crystallinity of 88.3% and thermal stability up to 170 °C (Table 1). On the other hand, CNF obtained by TEMPO oxidation from microcrystalline cellulose showed micrometric lengths and widths between 30 and 50 nm, with lower degrees of crystallinity than the CNC (66%) and higher thermal stability up to 225 °C. Table 1 shows the characteristics of the isolated materials, and Fig. S1 of the Supporting information shows TEM, DLS, TGA, DRX, and FTIR-ATR data.

The size, charge, crystallinity, and thermal stability of CNC and CNF (as listed in Table 1) lie within the ranges reported in the literature for similar materials [29,49-51]. As expected, CNCs have smaller sizes than CNFs while exhibiting higher crystallinity and a reduced amount of surface charges. The high amount of carboxylate units on NFC is reflected in a ζ -potential value of -59 mV for this material, in contrast with -39 mV for the CNC. The presence of surface charges (-SO₃⁻ or -COO⁻) prevents agglomeration – by Coulombic repulsions allowing the formation of stable aqueous dispersions of CNC and CNF.

The surface chemistry of nanocelluloses and their use as interfacially-active compounds depends on the type and number of polar groups at the surface. In our case, CNC has 117 mmol/kg of highly ionizable sulfate groups (pKa ~ 3.0) that can be utterly ionized at pH > 3. These groups are highly polar; however, due to their low

Table 1
CNC and CNF characterization.

| Parameter (Method) | CNC | CNF |
|--------------------------------------|---|---|
| Length (DLS) | | 100–250 nm |
| Width (TEM) | | 20–30 nm |
| |  |  |
| Surface charge (ζ -potential) | −39 mV | −59 mV |
| Surface groups (Conductimetry) | 117 mmol SO ₃ [−] /kg | 1200 mmol COOH/kg |
| Thermal stability (TGA) | 170 °C | 225 °C |
| Crystallinity Index (XRD) | 88.3% | 62.0% |
| Wettability (visual) | Water | Water |
| Theoretical HLB | 10.7 | 13.0 |

concentration on the surface of the CNC, they do not affect the theoretical HLB value to a great extent (10.7) [42,52]. On the other hand, CNF contains more ionizable groups (1200 mmol of COOH/kg) than CNC. In CNF, COOH units ($pK_a \sim 4.0$) are completely ionized (to the $-COO^-$ form) at the pH used in the tests (pH 6). Using hydrophilicity values for polar groups in CNC and CNF, we calculated the theoretical HLB using Eq. (1). The results were HLB values of 13.0 for CNF and 10.7 for CNC; these values correspond to hydrophilic (water soluble) o/w emulsifying agents. Interestingly, surface active agents used for stabilizing o/w emulsions can also act as destabilizers for w/o emulsions; thus we hypothesize that CNC and NFC can effectively be used as inhibitors of water-crude oil emulsions as demonstrated below [53,54].

3.2. Inhibition of emulsion formation with CNC and CNF in w/o model systems

Several authors agree that the process of formation of water-in-oil emulsions, in petroleum processing, involves the formation of a relatively rigid interfacial layer due to the presence of surface-active agents in the crude (polar species in asphaltenes, naphthenic acids). Therefore, avoiding w/o emulsion formation requires inhibiting agents that efficiently compete against naturally-present emulsifiers, preventing formation of the interfacial layer and allowing water separation [55,56]. The properties of nanocellulose particles (both nanocrystals and nanofibers) as surface active materials to stabilize emulsions, particularly of the oil-in-water kind, are abundantly illustrated in literature [57–62]. However, to the best of our knowledge, there are no reports regarding the use of nanocelluloses to destabilize water-in-crude oil emulsions, with current applications of these materials focused mostly on EOR processes as described in the introductory remarks.

We performed preliminary inhibition tests using a synthetic w/o emulsion made of commercial gasoline plus asphaltenes and a brine (pH 6) with a composition similar to that of the average formation water, as described in the Experimental section. When CNC was added to the brine before emulsion preparation, for final concentrations of 1000 to 5000 ppm, we were able to inhibit emulsion formation in all tests. Without CNC we obtained stable (up to six months) w/o emulsions. We lowered the amount of CNC for the inhibition test and found that no inhibition was observed for concentrations below 1000 ppm. Fig. 1 clearly illustrates the emulsion formation inhibition effect of adding CNC (1000 ppm) to the brine. In visual tests, we obtain a normalized water recovery of 80% assuming a total volume of the sample in the tube of 37.5 mL as seen in Fig. 1. Likewise, optical micrographs (bottom left) show a decrease in the amount of dispersed water in the organic phase of the sample with added CNC (1000 ppm) in contrast

with the control sample. Interestingly, we observe no significant change in water drop sizes upon CNC addition to the w/o emulsion; there is only change in their amount in the emulsion as seen in Fig. 1 (bottom left). Also, the remaining water in the organic phase is in the form of a water-in-oil dispersion ruling out a possible phase inversion when using CNC.

Emulsion formation and stability are complex processes at the molecular level; however, from a macroscopic perspective, these processes can be studied by following variations in optical characteristics of opaque dispersions. To assess emulsion stability, we followed changes over time in the Instability Index (TSI), a statistical parameter calculated from variations in the backscattering intensity of NIR radiation interacting with the sample, relative to the original. High values of TSI indicate phase separation, which translates into low emulsion stability in the case of w/o emulsions. Fig. 1 (top right) shows the global TSI vs. time plot for the control emulsion and the emulsions prepared with CNC. The TSI plateaus at five after 20 min for the control sample, indicating a highly stable emulsion.

In contrast, the sample with CNC (1000 ppm) exhibits a maximum TSI value of 30 after 100 min, indicating complete phase separation in agreement with the visual tests. Interestingly, when following only backscattering changes in the lower part of the sample vial (where the aqueous phase collects in case of phase separation), we observe dramatic changes in the TSI values for the sample with CNC (1000 ppm). A maximum TSI value of 120, plateauing after 70 min for the aqueous phase, indicates fast destabilization kinetics and rapid phase separation, in other words, low emulsion stability.

As reported by Djuve *et al.* [63], an emulsion inhibitor must compete with natural surfactants, draining them from the interfacial layer and decreasing the surface tension gradient so that breaking or inhibiting emulsion formation occurs. In the model emulsions we prepared, the asphaltenes act as surface-active compounds forming an interfacial film and stabilizing the emulsion for several months. Such was the case of the control emulsion, which remained stable for more than six months. When the CNC was added to the aqueous medium, in concentrations above 1000 ppm, emulsion formation was hindered as a consequence of dynamic interactions between the CNC and the surface-active compounds in asphaltenes.

Using the same w/o model emulsion system described above, we performed inhibition tests using CNF. As with CNC, when CNF was added to the brine before emulsion preparation, for final concentrations of 1500 to 5000 ppm, we were able to inhibit emulsion formation in all tests. Without CNF we obtained stable (up to six months) w/o emulsions. We lowered the amount of CNF and found that the inhibition concentration threshold was 1500 ppm, below which w/o emulsions

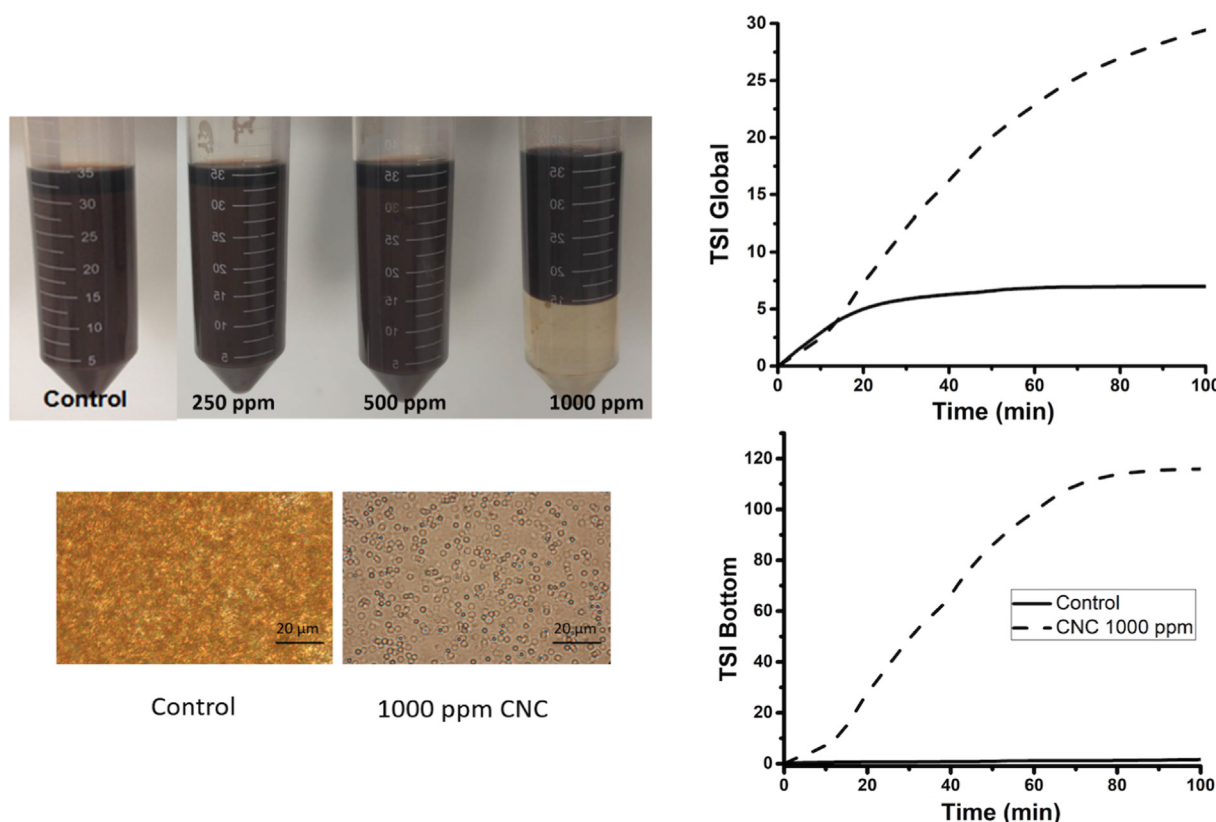


Fig. 1. Emulsion inhibition effects for CNC: visual tests (top left), optical micrographs of the control emulsion and the aqueous layer for the sample with 1000 ppm of CNC (bottom left); backscattering NIR measurements featuring the dynamics of the instability indexes for the overall mixture (top right) and the aqueous layer (bottom right).

were readily formed. In Fig. 2 the visual tests (top left) we obtain a normalized water recovery of 77.8%.

Optical micrographs (bottom left) indicate decrease amount of water in the final dispersion after CNF addition; however, there is a significant increase in water droplet size with CNF when compared to the same experiment with CNC. Fig. 2 (top right) shows the global TSI vs. time plot for the control emulsion and the emulsion prepared with 1500 ppm of CNF. The TSI slowly rises to 4.2 after 100 min for the control sample, indicating a stable emulsion. In contrast, the sample with CNF (1500 ppm) becomes steadily unstable after 100 min, indicating phase separation. The backscattering dynamics in the lower part of the sample vial (where the aqueous phase collects in case of phase separation) show a more accurate picture than the TSI global. A maximum TSI value for the aqueous phase of 25, plateauing after 70 min, indicates a fast destabilization and rapid phase separation with CNF, in other words, low emulsion stability.

To establish the distribution of CNF we studied the phases formed during the inhibition test using optical microscopy. The CNF tested in our work have negatively charged surfaces, due to the presence of carboxylate groups, thus we selected Methylene Blue (a cationic dye) as label to observe the distribution of the cellulosic material in the mixture. Fig. 3 shows optical images of the aqueous, organic, and interfacial layers five minutes after mixing the phases with the high shear mixer, note that the amount of asphaltenes in this particular experiment was reduced to facilitate light transmission. The characteristic blue color of MB was observed in the aqueous and interfacial layers. When zooming at the interfacial layer, we noticed that the boundary of the water/oil interface was tinted blue. This observation indicates that CNF is preferably located at the interfacial water/oil film. Interestingly, several investigations dealing with the use of high molecular weight surfactants with abundant oxygen-containing moieties agree in that these materials can alter the interfacial water/oil film rheology

promoting coalescence and sedimentation [68]. We believe that, along the same lines, highly hydrophilic nanocelluloses, with abundant oxygen atoms, high-molecular-weight, and high HLB values, can also efficiently inhibit w/o emulsion formation by migrating to the w/o interface as seen in Fig. 3.

On the other hand, as mentioned above, the type of emulsion and its stability are related to the surfactants hydrophilic/hydrophobic nature [64], with mildly polar surfactants such as asphaltenes tending to stabilize w/o emulsions, while CNC or CNF of a strongly hydrophilic nature tend to either stabilize o/w emulsions or even act as solubilizing agents. Therefore, adding CNC or CNF to the water before emulsion formation can efficiently hinder stabilization of water droplets in the oil phase by competing with natural surfactants. According to reports by Rondón *et al.* [65,66], an efficient w/o demulsifier must have different properties to those of the surfactants that stabilize the w/o emulsion. An efficient w/o emulsifier must be then highly hydrophilic (such as CNC and CNF with HLB of 10.7 and 13, respectively) since the surfactants stabilizing the emulsion (asphaltenes) have low hydrophilicity when compared with CNC.

3.3. Inhibition of emulsion formation with CNC in w/Crude oil dispersions

3.3.1. Light crude oil

We hypothesize that CNC, smaller and less hydrophilic than CNF, can migrate easily to the w-o interface hindering emulsion formation. According to their HLB values, CNC (10.7) and CNF (13.0) qualify as o/w emulsion stabilizers and also as w/o emulsions destabilizers. However, CNC is slightly less hydrophilic than CNF, due to a lower amount of sulfate groups. Also, CNC has higher mobility than CNF due to its size. Thus, we selected CNC for further testing as emulsion inhibitors in w/o dispersions prepared using a light crude oil (API: 31.7°).

In real-world situations, the success of a formulation to inhibit

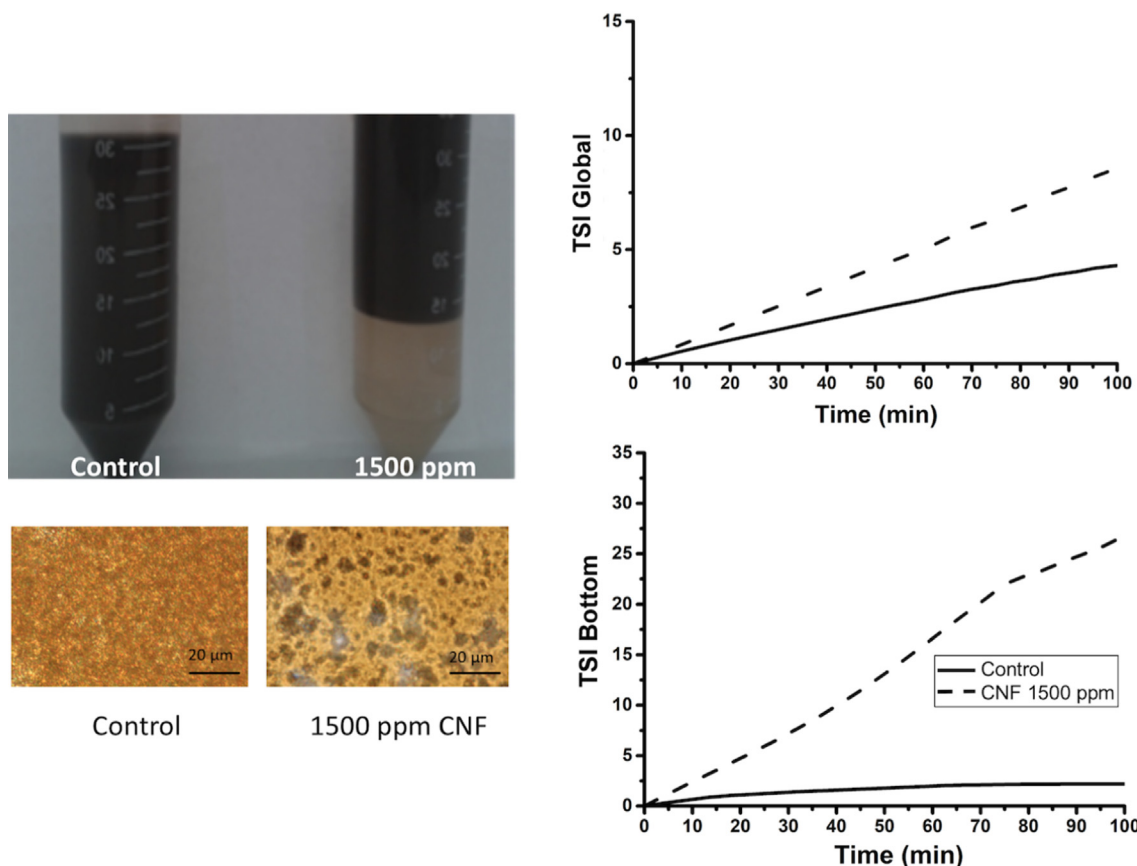


Fig. 2. Emulsion inhibition effects for CNF: visual tests (top left), optical micrographs of the control emulsion and the aqueous layer for the sample with 1500 ppm of CNF (bottom left); backscattering NIR measurements featuring the dynamics of the instability indexes for the overall mixture (top right) and the aqueous layer (bottom right).

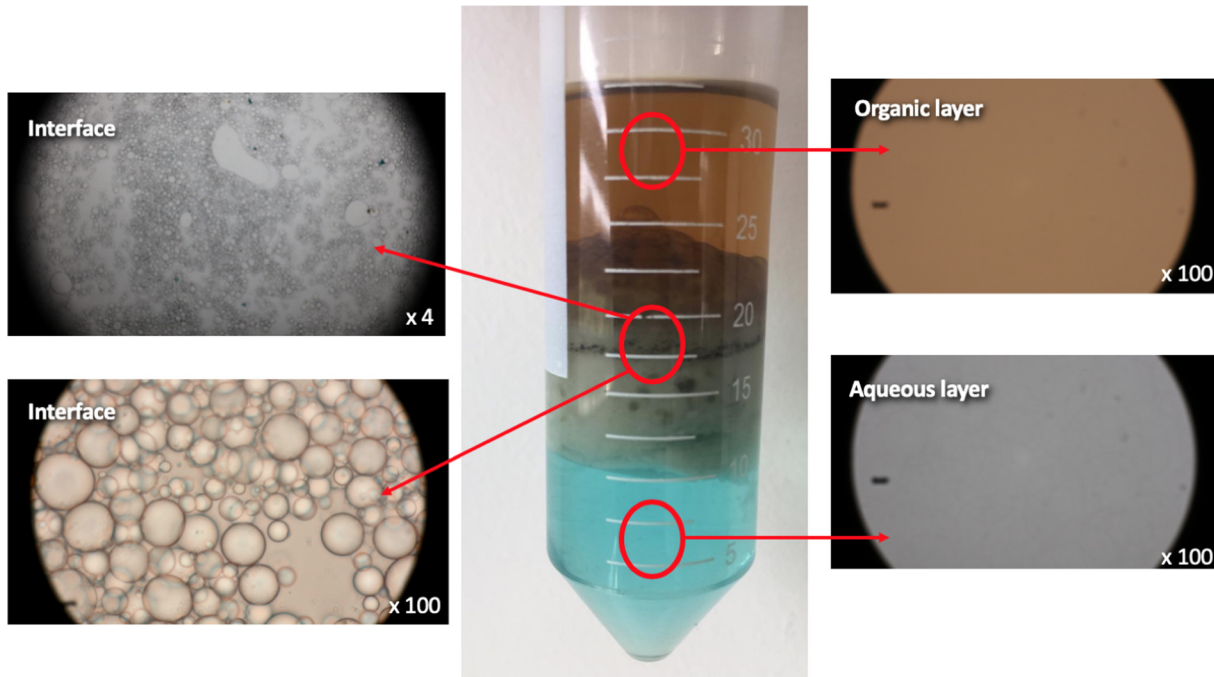


Fig. 3. Optical microscopy images of the organic aqueous and interfacial layers observed during an inhibition test with CNF, using Methylene Blue (cationic dye) as a label for cellulose.

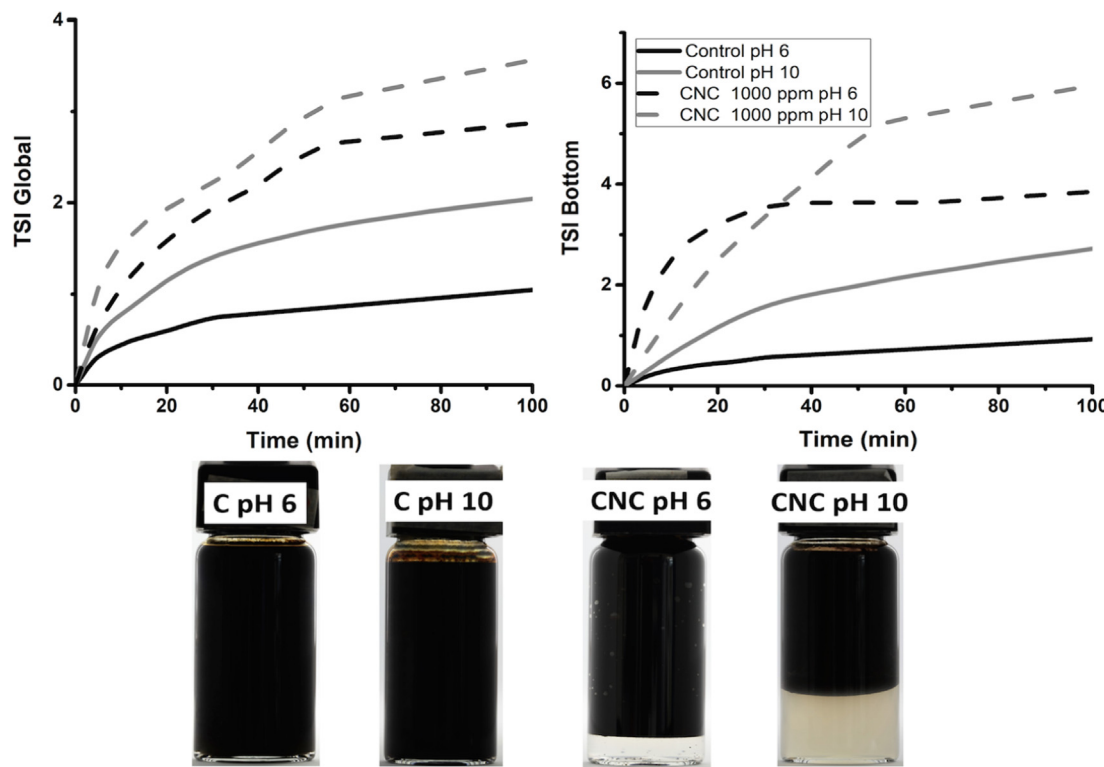


Fig. 4. Inhibition tests for a water-in-light crude oil emulsion with suspensions of 1000 ppm of CNC in 1000 ppm NaCl brines at pH 6 and 10.

emulsion formation does not only depend on the nature of the surfactant but also on factors such as pH, temperature, and water salinity [65]. Therefore, we varied experimental conditions to test the effect of pH and salinity on emulsion inhibition by CNC. To determine pH influence on emulsion inhibition we carried out tests mixing a light crude oil with CNC suspensions (1000 ppm) in various brines (1000, 6000, and 12000 ppm NaCl) at pH 6 and 10. Starting with 1000 ppm NaCl brines, the optical images in Fig. 4 clearly show more water recovery at pH 10 (70%) than at pH 6 (25%). No water was recovered from the control experiments (where CNC was not added to the brine). Both global and bottom TSI graphs show the same backscattering behavior for the control mixtures, supporting the visual assessment of no phase separation occurring in these samples.

On the other hand, the global TSI profiles for the samples with CNC show increased destabilization with time. However, the effect is more evident if we examine the TSI bottom corresponding to the lower part of the vial where the free water is observed. Increasing the CNC carrier fluid pH has a significant effect on emulsion destabilization (higher TSI values), while a low pH does not promote significant water recovery (lower TSI values). pH plays an essential role in the emulsion inhibition process by modulating surface charge density on CNC. The higher the pH, the more superficial charges available for interaction with water and to promote coalescence and separation of the aqueous phase. Interestingly, the water recovery in these closer-to-real systems is slightly lower than the observed recoveries in model systems (see above) implying that CNC can not only compete with the asphaltenes but also with other natural surfactants present in the crude, promoting coalescence of water droplets and inducing phase separation.

For brines with 6000 ppm of NaCl, optical images in Fig. 5 show minimal water recovery at pH 10 (10%) and pH 6 (25%). No water was recovered from the control experiments (where CNC was not added to the brine). Both global and bottom TSI graphs show the same backscattering behavior for the control mixtures, supporting the visual assessment of no phase separation occurring in these samples. Increasing dissolved ions in the water dramatically affects the performance of CNC

as emulsion inhibitor. Also, increasing salt concentration up to 12000 ppm results in similar behavior than with 6000 ppm (See Fig. S3 in the Supporting Information section).

Up to this point, when using CNC as emulsion inhibitor, we observed the highest efficiency at pH 10 and 1000 ppm of NaCl in the aqueous phase. CNC has a high surface charge as a result of sulfate groups; at pH 10 these groups are entirely ionized making CNC highly active towards the aqueous interface where it can displace or counteract natural emulsifiers naturally present in the crude oil.

3.3.2. Heavy crude oil

Selecting an appropriate emulsion breaker/inhibitor is not an easy task, and there is currently no “one size fits all” solution. Literature reports indicate the choice depends on many variables such as crude oil composition, properties, and formation water composition, among others. Thus, we wanted to determine whether or not CNC could be used as an inhibitor for both water-in-oil emulsions of light and heavy oils.

Fig. 6 shows the instability index for a water-in-heavy crude oil (API 14.7) emulsion prepared with a NaCl brine (1000 ppm); the dispersion is stable for several months. Addition of CNC (1000 ppm) to the water before emulsion formation results in dramatic instability. Up to 60% of water release is observed during the first 20 min of the stability test, as seen in Fig. 6.

In the graphs for global destabilization we observed an increase of the TSI, up to 10 for the emulsion prepared with the CNC, this behavior indicates a destabilization process induced by the nanocrystals, while in the control emulsion of this crude there is no significant change in the TSI, indicating high stability. TSI values in the lower part of the test vial are much higher, 40 for the emulsion prepared with CNC; this is consistent with the amount of water recovered in this experiment (60%). This tests, using real crude oil, show that the CNC can compete efficiently with the different surfactants present in the sample, as expected the degree of inhibition depends on the type of crude oil and the characteristics of the brine.

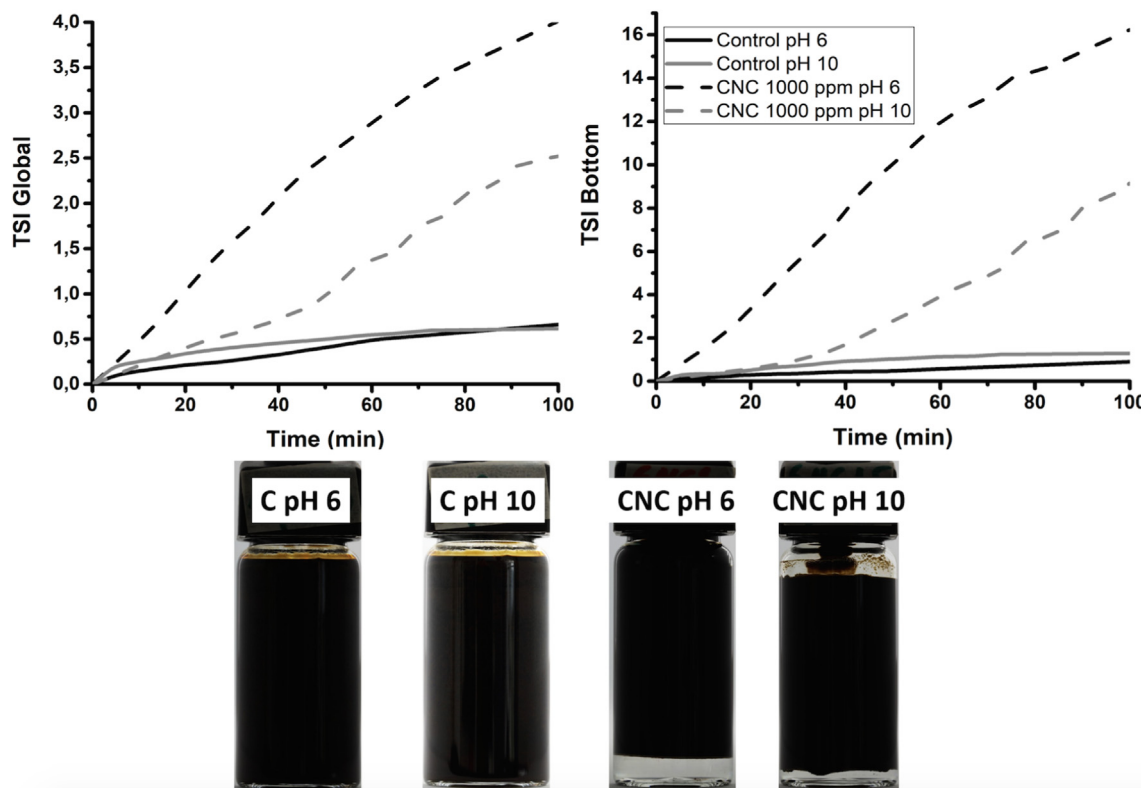


Fig. 5. Inhibition tests for a water-in-light crude oil emulsion with suspensions of 1000 ppm CNC in brines of 6000 ppm NaCl at pH 6 and 10.

4. Conclusions

CNC and CNF behavior at interfaces depends on two key parameters: surface chemistry and particle structure. The ionic groups present in the surface of nanocelluloses (SO_3^- in CNC and COOH^- in CNF) give these materials affinity for polar phases, while their shape allows them to diffuse efficiently in solution. We observe significant emulsion inhibition behavior with both CNC and CNF; however, CNC can be used at lower concentrations. An efficient emulsion inhibitor must compete with natural surfactants, draining them from the interfacial layer and decreasing the surface tension gradient so that breaking or inhibiting emulsion formation occurs [67]. CNC can efficiently disrupt or inhibit the formation of a stable interfacial layer upon water interaction with surface-active compounds present in light and heavy crude oils.

From an economic perspective, the nanocelluloses (NCCs) market is

fast growing due to their many applications. NCCs are biodegradable, biocompatible, non-toxic, and carbon neutral materials with outstanding mechanical, thermal, and physicochemical properties. Currently, NCCs are used by the paints and coatings, oil and gas, cosmetics and pharma, and food and beverage industries. The fastest growing market for NCCs is Asia, and many well established companies such as CelluForce, American Process Inc., Melodea Ltd, Chuetsu Pulp and Paper, Nippon Paper Industries Co. Ltd, and Borregaard, among others, are able to produce NCCs in industrial quantities.

However, the market for NCCs does not have enough traction and the production prices are still very high, when compared with materials with similar characteristics from petrochemical sources. Lowering NCCs prices depend on finding widespread applications for the materials. The oil industry, with the highest CO_2 footprint in the planet, is a suitable candidate for NCCs applications. With current fossil fuel reserves switching to heavy oils, demulsifiers and non-emulsifiers consumption

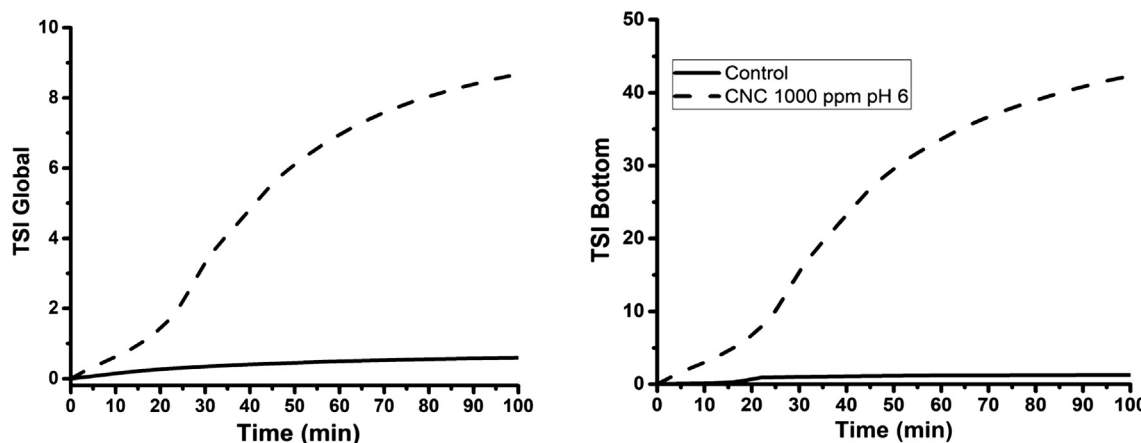


Fig. 6. Inhibition tests for a water-in-heavy crude oil emulsion with suspensions of 1000 ppm CNC in brines of 1000 ppm NaCl at pH 10.

will increase at an accelerated pace. According to a recent study, the demulsifier market will be worth 2.53 Billion USD by 2022. With this forecast in mind, there is space, from our point of view, for alternative carbon-neutral materials (such as NCCs) in this particular market.

CRediT authorship contribution statement

Maria M. González: Investigation, Writing - original draft, Visualization. **Cristian Blanco-Tirado:** Conceptualization, Funding acquisition. **Marianny Y. Combariza:** Conceptualization, Formal analysis, Writing - review & editing, Supervision.

Acknowledgments

The authors acknowledge technical support from Guatiguará's Tech Park Research Facility-Universidad Industrial de Santander, Colombia and ECOPETROL S.A. (Grant No. 03-5211794). Additionally, we thank the collaboration of the staff of the NMR, XRD, and Microscopy laboratories of the Industrial University of Santander. MMGB thanks Departamento Administrativo de Ciencia, Tecnología e Innovación COLCIENCIAS (Program 727-2016) for a scholarship. We also thank Professor Juan Hinestroza director of the Textiles Nanotechnology Lab, College of Human Ecology, Cornell University for TEM analyses and discussion; we also acknowledge use of the Cornell Center for Materials Research Shared Facilities which are supported through the NSF MRSEC program (DMR-1719875) and an INVEST grant via the Cornell Center for Materials Research (M01-1985) for TEM analyses.

Appendix A. Supplementary data

Supplementary data to this article can be found online at <https://doi.org/10.1016/j.fuel.2019.116830>.

References

- [1] Kokal S. Crude oil emulsions: a state-of-the-art review. *Proc. SPE Annu. Tech. Conf. Exhib.* 2002;11. <https://doi.org/10.2118/77497-MS>.
- [2] Salam KK, Alade AO, Arinkoola AO, Opawale A. Improving the demulsification process of heavy crude oil emulsion through blending with diluent. *J Pet Eng* 2013;1–6. 2013.
- [3] Wen Y, et al. Analysis of biological demulsification process of water-in-oil emulsion by Alcaligenes sp. S-XJ-1. *Bioresour. Technol.* 2010;101:8315–22.
- [4] Lemarchanda Caroline, Couvreur Patrick, Vauthier Christine, Dominique Costantini RG. 'Study of emulsion stabilization by graft copolymers using the optical analyzer Turbiscan. *Colloids and Surfaces A: Physicochemical and Engineering Aspects* Elsevier Ltd; 2015. p. 2–18. <https://doi.org/10.1016/j.copbio.2016.01.002>.
- [5] Dalmazzone C, Bocard C, Ballerini D. IFP methodology for developing water-in-crude oil emulsion inhibitors. *Spill Sci Technol Bull* 1995;2:143–50. [https://doi.org/10.1016/S1353-2561\(96\)00013-8](https://doi.org/10.1016/S1353-2561(96)00013-8).
- [6] Hjartnes TN, Sørland GH, Simon S, Sjöblom J. Demulsification of crude oil emulsions tracked by pulsed field gradient (PFG) nuclear magnetic resonance (NMR). Part I: chemical demulsification. *Ind Eng Chem Res* 2019;58:2310–23. <https://doi.org/10.1021/acs.iecr.8b05165>.
- [7] Cheng Q, Ye D, Chang C, Zhang L. Facile fabrication of superhydrophilic membranes consisted of fibrous tunicate cellulose nanocrystals for highly efficient oil/water separation. *J Memb Sci* 2017;525:1–8. <https://doi.org/10.1016/j.memsci.2016.11.084>.
- [8] Roodbari NH, Badie A, Soleimani E, Khaniani Y. Tweens demulsification effects on heavy crude oil/water emulsion. *Arab J Chem* 2016;9:S806–11. <https://doi.org/10.1016/j.arabjc.2011.08.009>.
- [9] Abdul Khalil HPS, Davoudpour Y, Islam MN, Mustapha A, Sudesh K, Dungani R, et al. Production and modification of nanofibrillated cellulose using various mechanical processes: a review. *Carbohydr Polym* 2014;99:649–65. <https://doi.org/10.1016/j.carbpol.2013.08.069>.
- [10] Abraham, E., Deepa, B., Pothan, L. a., Jacob, M., Thomas, S., Cvelbar, U., & Anandjiwala, R. (2011). Extraction of nanocellulose fibrils from lignocellulosic fibres: A novel approach. *Carbohydrate Polymers*, 86(4), 1468–1475. <http://doi.org/10.1016/j.carbpol.2011.06.034>.
- [11] Beck-Candanedo S, Roman M, Gray DG. Effect of reaction conditions on the properties and behavior of wood cellulose nanocrystal suspensions. *Biomacromolecules* 2005;6:1048–54. <https://doi.org/10.1021/bm049300p>.
- [12] Isogai A, Saito T, Fukuzumi H. TEMPO-oxidized cellulose nanofibers. *Nanoscale* 2011;3(1):71–85. <https://doi.org/10.1039/c0nr00583e>.
- [13] Bondeson D, Mathew A, Oksman K. Optimization of the isolation of nanocrystals from microcrystalline cellulose by acid hydrolysis. *Cellulose* 2006;13(2):171–80. <https://doi.org/10.1007/s10570-006-9061-4>.
- [14] Saito T, Kimura S, Nishiyama Y, Isogai A. Cellulose nanofibers prepared by TEMPO-mediated oxidation of native cellulose. *Biomacromolecules* 2007;8(8):2485–91. <https://doi.org/10.1021/bm0703970>.
- [15] Habibi Y, Lucia LA, Rojas OJ. Cellulose nanocrystals: Chemistry, self-assembly, and applications. *Chem Rev* 2010;110(6):3479–500. <https://doi.org/10.1021/cr900339w>.
- [16] Korhonen JT, Kettunen M, Ras RHA, Ikkala O. Hydrophobic nanocellulose aerogels as floating, sustainable, reusable, and recyclable oil absorbents. *ACS Appl Mater Interfaces* 2011;3(6):1813–6. <https://doi.org/10.1021/am200475b>.
- [17] Qiu X, Hu S. "Smart" materials based on cellulose: A review of the preparations, properties, and applications. *Materials* 2013. <https://doi.org/10.3390/ma6030738>.
- [18] Hubbe, M. a., Rojas, O. J., Lucia, L. a. and Sain, M. (2008) 'Cellulosic Nanocomposites: a Review', *BioResources*, 3(3), pp. 929–980. doi: 10.15376/biores.3.3.929-980.
- [19] Andresen, M., & Stenius, P. (n.d.). Water-in-oil emulsions stabilized by hydrophobized microfibrillated cellulose. *Journal of Dispersion Science and Technology*, 28(6), 844–851. Retrieved from <http://cat.inist.fr/?aModele=afficheN&cpsidt=19120733>.
- [20] Lif A, Stenstad P, Syverud K, Nydén M, Holmberg K. Fischer-Tropsch diesel emulsions stabilised by microfibrillated cellulose and nonionic surfactants. *J Colloid Interface Sci* 2010;352(2):585–92. <https://doi.org/10.1016/j.jcis.2010.08.052>.
- [21] Hou J, Feng X, Masliyah J, Xu Z. *Understanding Interfacial Behavior of Ethylcellulose. Bitumen Interface*; 2012.
- [22] Zoppe, J. O., Venditti, R. A. and Rojas, O. J. (2012) 'Pickering emulsions stabilized by cellulose nanocrystals grafted with thermo-responsive polymer brushes', *J. Colloid Interface Sci. Elsevier Inc.*, 369(1), pp. 202–209. doi: 10.1016/j.jcis.2011.12.011.
- [23] Cunha AG, Mougel JB, Cathala B, Berglund LA, Capron I. Preparation of double pickering emulsions stabilized by chemically tailored nanocelluloses. *Langmuir* 2014;30(31). <https://doi.org/10.1021/la5017577>.
- [24] Fujisawa S, Togawa E, Kuroda K. Nanocellulose-stabilized Pickering emulsions and their applications. *Sci Technol Adv Mater* 2017;18:959–71. <https://doi.org/10.1080/14686996.2017.1401423>.
- [25] Kalashnikova I, et al. Modulation of cellulose nanocrystals amphiphilic properties to stabilize oil/water interface (supporting info). *Biomacromolecules* 2012;13(1):267–75. <https://doi.org/10.1017/CBO9781107415324.004>.
- [26] Li X, Li J, Gong J, Kuang Y, Mo I, Song T. Cellulose nanocrystals (CNCs) with different crystalline allomorph for oil in water Pickering emulsions. *Carbohydr Polym* 2018;183:303–310. <https://doi.org/10.1016/j.carbpol.2017.12.085>.
- [27] Niu F, Han B, Fan J, Kou M, Zhang B, Feng Z-J, et al. Characterization of structure and stability of emulsions stabilized with cellulose macro/nanoparticles. *Carbohydr Polym* 2018;199:314–9. <https://doi.org/10.1016/j.carbpol.2018.07.025>.
- [28] Gestrañiu M, Stenius P, Kontturi E, Sjöblom J, Tammelin T. Phase behavior and droplet size of oil-in-water Pickering emulsions stabilised with plant-derived nanocellulosic materials. *Colloids Surfaces A Physicochem Eng Asp* 2017;519:60–70. <https://doi.org/10.1016/j.colsurfa.2016.04.025>.
- [29] Li Y, Wang B, Ma W, Wang B. Review of Recent Development on Preparation, Properties, and Applications of Cellulose-Based Functional Materials. *Int J Polym Sci* 2018. <https://doi.org/10.1155/2018/8973643>.
- [30] Li Q, Wei B, Lu L, Li Y, Wen Y, Pu W, et al. Investigation of physical properties and displacement mechanisms of surface-grafted nano-cellulose fluids for enhanced oil recovery. *Fuel* 2017;207:352–64. <https://doi.org/10.1016/j.fuel.2017.06.103>.
- [31] Wei B, Li Q, Jin F, Li H, Wang C. The potential of a novel nanofluid in enhancing oil recovery. *Energy Fuels* 2016;30:2882–91. <https://doi.org/10.1021/acs.energyfuels.6b00244>.
- [32] Aoudia M, Al-Shibli MN, Al-kasimi LH, Al-maamari R, Al-Bemani A. Novel Surfactants for Ultralow Interfacial Tension in a Wide Range of Surfactant Concentration and Temperature 2006;9:287–93.
- [33] Li Q, Wei B, Xue Y, Wen Y, Li J. Improving the physical properties of nano cellulose through chemical grafting for potential use in enhancing oil recovery. *J Bioreour Bioprod* 2016;1:186–91.
- [34] Wei B, Li H, Li Q, Wen Y, Sun L, Wei P, et al. Stabilization of foam lamella using novel surface-grafted nanocellulose-based nanofluids. *Langmuir* 2017;33:5127–39. <https://doi.org/10.1021/acs.langmuir.7b00387>.
- [35] Wei B, Wang Y, Wen Y, Xu X, Wood C, Sun L. Bubble breakup dynamics and flow behaviors of a surface-functionalized nanocellulose based nanofluid stabilized foam in constricted microfluidic devices. *J Ind Eng Chem* 2018;68:24–32. <https://doi.org/10.1016/j.jiec.2018.07.025>.
- [36] Molnes SN, Mamoun A, Paso KG, Strand S, Syverud K. Investigation of a new application for cellulose nanocrystals: a study of the enhanced oil recovery potential by use of a green additive. *Cellulose* 2018;25:2289–301. <https://doi.org/10.1007/s10570-018-1715-5>.
- [37] Molnes SN, Torrijos IP, Strand S, Paso KG, Syverud K. Sandstone injectivity and salt stability of cellulose nanocrystals (CNC) dispersions—Premises for the use of CNC in enhanced oil recovery. *Ind Crops Prod* 2016;93:152–60. <https://doi.org/10.1016/j.indcrop.2016.03.019>.
- [38] Molnes SN, Paso KG, Strand S, Syverud K. The effects of pH, time and temperature on the stability and viscosity of cellulose nanocrystal (CNC) dispersions: implications for use in enhanced oil recovery. *Cellulose* 2017;24:4479–91. <https://doi.org/10.1007/s10570-017-1437-0>.
- [39] Fujisawa S, Okita Y, Fukuzumi H, Saito T, Isogai A. Preparation and characterization of TEMPO-oxidized cellulose nanofibril films with free carboxyl groups. *Carbohydr Polym* Elsevier Ltd. 2011;84(1):579–83. <https://doi.org/10.1016/j.carbpol.2010.12.029>.
- [40] Abitbol T, Kloser E, Gray DG. Estimation of the surface sulfur content of cellulose

nanocrystals prepared by sulfuric acid hydrolysis. *Cellulose* 2013;20(2):785–94. <https://doi.org/10.1007/s10570-013-9871-0>.

[41] Habibi Y, Chanzy H, Vignon MR. TEMPO-mediated surface oxidation of cellulose whiskers. *Cellulose* 2006;13(6):679–87. <https://doi.org/10.1007/s10570-006-9075-y>.

[42] Davies JT. Emulsion Type. I. Physical Chemistry of Gas/Liquid/Liq Interfaces 1957;426–38.

[43] Maaref S, Ayatollahi S. The effect of brine salinity on water-in-oil emulsion stability through droplet size distribution analysis: A case study. *J Dispers Sci Technol* 2018;39:721–33. <https://doi.org/10.1080/01932691.2017.1386569>.

[44] Giraldo-Dávila, D., Chacón-Patiño, M. L., McKenna, A. M., Blanco-Tirado, C. and Combariza, M. Y. (2018) 'Correlations between Molecular Composition and Adsorption, Aggregation, and Emulsifying Behaviors of PetroPhase 2017 Asphaltenes and Their Thin-Layer Chromatography Fractions', *Energy & Fuels*, p. acs.energyfuels.7b02859. doi: 10.1021/acs.energyfuels.7b02859.

[45] Kang W, Xu B, Wang Y, Li Y, Shan X, An F, et al. Stability mechanism of W/O crude oil emulsion stabilized by polymer and surfactant. *Colloids Surfaces A: Physicochem Eng Aspects Elsevier B.V.* 2011;384(1–3):555–60. <https://doi.org/10.1016/j.colsurfa.2011.05.017>.

[46] Aveyard R, Binks BP, Clint JH. Emulsions stabilised solely by colloidal particles. *Adv Colloid Interface Sci* 2003;100–102:503–46. [https://doi.org/10.1016/S0001-8686\(02\)00069-6](https://doi.org/10.1016/S0001-8686(02)00069-6).

[47] Leal-Calderon F, Schmitt V. Solid-stabilized emulsions. *Curr Opin Colloid Interface Sci* 2008;13:217–27. <https://doi.org/10.1016/j.cocis.2007.09.005>.

[48] Johnson RK, Zink-Sharp A, Glasser WG. Preparation and characterization of hydrophobic derivatives of TEMPO-oxidized nanocelluloses. *Cellulose* 2011;18:1599–609. <https://doi.org/10.1007/s10570-011-9579-y>.

[49] Roman M, Winter WT. Effect of sulfate groups from sulfuric acid hydrolysis on the thermal degradation behavior of bacterial cellulose. *Biomacromolecules* 2004;5:1671–7. <https://doi.org/10.1021/bm034519+>.

[50] Lu P, Hsieh Y-L. Preparation and properties of cellulose nanocrystals: Rods, spheres, and network. *Carbohydr Polym* 2010;82:329–36. <https://doi.org/10.1016/j.carbpol.2010.04.073>.

[51] Jonoobi M, Oladi R, Davoudpour Y, Oksman K, Dufresne A, Hamzeh Y, et al. Different preparation methods and properties of nanostructured cellulose from various natural resources and residues: a review. *Cellulose* 2015;22. <https://doi.org/10.1007/s10570-015-0551-0>.

[52] Guo X, Rong Z, Ying X. Calculation of hydrophilic-lipophile balance for polyethoxylated surfactants by group contribution method. *J Colloid Interface Sci* 2006;298:441–50. <https://doi.org/10.1016/j.jcis.2005.12.009>.

[53] Xia L, Lu S, Cao G. Stability and demulsification of emulsions stabilized by asphaltenes or resins. *J Colloid Interface Sci* 2004;271(2):504–6. <https://doi.org/10.1016/j.jcis.2003.11.027>.

[54] Oliveira PF, Santos ICVM, Vieira HVP, Fraga AK, Mansur CRE. Interfacial rheology of asphaltene emulsions in the presence of nanoemulsions based on a polyoxide surfactant and asphaltene dispersant. *Fuel Elsevier Ltd* 2017;193:220–9. <https://doi.org/10.1016/j.fuel.2016.12.051>.

[55] Ortiz, D. P., Baydak, E. N. and Yarranton, H. W. (2010) 'Effect of surfactants on interfacial films and stability of water-in-oil emulsions stabilized by asphaltenes,' *Journal of Colloid and Interface Science*. Elsevier Inc., 351(2), pp. 542–555. doi: 10.1016/j.jcis.2010.08.032.

[56] Abdurahman, N. H., and Mahmood, W. K. (2012) 'Stability of water-in-crude oil emulsions: Effect of cocamide diethanolamine (DEA) and Span83', *Int. J. Phys. Sci.*, 7(41), pp. 5585–5597. doi: 10.5897/IJPS12.405.

[57] Capron I, Rojas OJ, Bordes R. Behavior of nanocelluloses at interfaces. *Curr Opin Colloid Interface Sci* 2017;29:83–95. <https://doi.org/10.1016/j.cocis.2017.04.001>.

[58] Brinchi L, Cotana F, Fortunati E, Kenny JM. Production of nanocrystalline cellulose from lignocellulosic biomass: technology and applications. *Carbohydr Polym* 2013;94:154–69. <https://doi.org/10.1016/j.carbpol.2013.01.033>.

[59] Ojala J, Sirviö JA, Liimatainen H. Nanoparticle emulsifiers based on bifunctionalized cellulose nanocrystals as marine diesel oil-water emulsion stabilizers. *Chem Eng J* 2016;288:312–20. <https://doi.org/10.1016/j.cej.2015.10.113>.

[60] Buffiere J, Balogh-Michels Z, Borrega M, Geiger T, Zimmermann T, Sixta H. The chemical-free production of nanocelluloses from microcrystalline cellulose and their use as Pickering emulsion stabilizer. *Carbohydr Polym* 2017;178:48–56. <https://doi.org/10.1016/j.carbpol.2017.09.028>.

[61] Mikulcová V, Bordes R, Kašpárová V. On the preparation and antibacterial activity of emulsions stabilized with nanocellulose particles. *Food Hydrocoll* 2016;61:780–92. <https://doi.org/10.1016/j.foodhyd.2016.06.031>.

[62] Laitinen O, Ojala J, Sirviö JA, Liimatainen H. Sustainable stabilization of oil in water emulsions by cellulose nanocrystals synthesized from deep eutectic solvents. *Cellulose* 2017;24:1679–89. <https://doi.org/10.1007/s10570-017-1226-9>.

[63] Djuve J, Yang X, Fjellanger IJ, Sjöblom J, Pelizzetti E. Chemical destabilization of crude oil based emulsions and asphaltene stabilized emulsions. *Colloid Polym Sci* 2001;279(3):232–9. <https://doi.org/10.1007/s003960000413>.

[64] Fan Y, Simon S, Sjöblom J. Chemical destabilization of crude oil emulsions: Effect of nonionic surfactants as emulsion inhibitors. *Energy Fuels* 2009;23(9):4575–83. <https://doi.org/10.1021/ef900355d>.

[65] Rondón M, Pereira JC, Bouriat P, Gracia A, Lachaise J, Salager JL. Breaking of water-in-crude oil emulsions. 2. Influence of asphaltene concentration and diluent nature on demulsifier action. *Energy Fuels* 2008;22(2):702–7. <https://doi.org/10.1021/ef7003877>.

[66] Rondón M, Bouriat P, Lachaise J, Salager JL. Breaking of water-in-crude oil emulsions. 1. Physicochemical phenomenology of demulsifier action. *Energy Fuels* 2006;20(4):1600–4. <https://doi.org/10.1021/ef0600170>.

[67] Kumar K, Nikolov AD, Wasan DT. Mechanisms of Stabilization of Water-in-Crude Oil Emulsions. *Ind Eng Chem Res* 2001;40:3009–14. <https://doi.org/10.1021/ie000663p>.

[68] Wang J, Hu F-L, Li C-Q, Li J, Yang Y. Synthesis of dendritic polyether surfactants for demulsification. *Sep Purif Technol* 2010;73(3):349–54.